

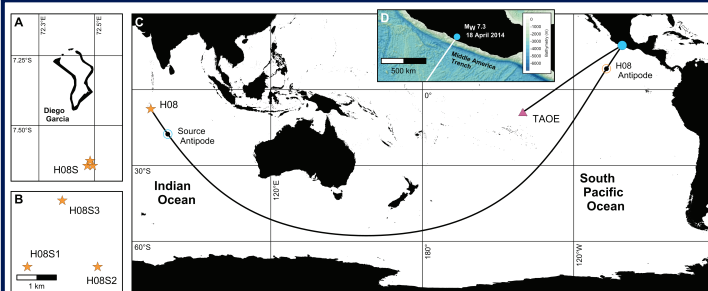


Abstract

Large-scale tectonic earthquakes occur regularly along the northern Middle America Trench, a major subduction zone located offshore the Pacific coast of Mexico. Time-difference-of-arrival calculations suggest that low-frequency acoustic phases generated by these events couple into the Sound Fixing and Ranging (SOFAR) channel and can be recorded as far as Diego Garcia, Indian Ocean, where a hydrophone triplet array (H08S) is operated as part of the International Monitoring System (IMS). At more than ~21,300 km, source-receiver distances exceed the antipodal range, making them the furthest artificial or naturally occurring underwater signals to have ever been observed on Earth [cf. *Heaney et al., 1991; Metz et al., 2016*].

Here, we investigate T phase arrivals from the 2014 Guerrero earthquake as an example of suprapodal acoustic propagation. Preliminary findings are consistent with observations at regional broadband stations and two dimensional, parabolic equation modelling, highlighting the exceptional capabilities of the IMS hydroacoustic waveform component and its potential for remotely detecting seismic activity. Nonetheless, suprapodal T phase arrivals recorded at H08S are not normally associated with their respective event origin in the automated or reviewed branches of the IDC catalogue (SEL3 and REB, respectively).

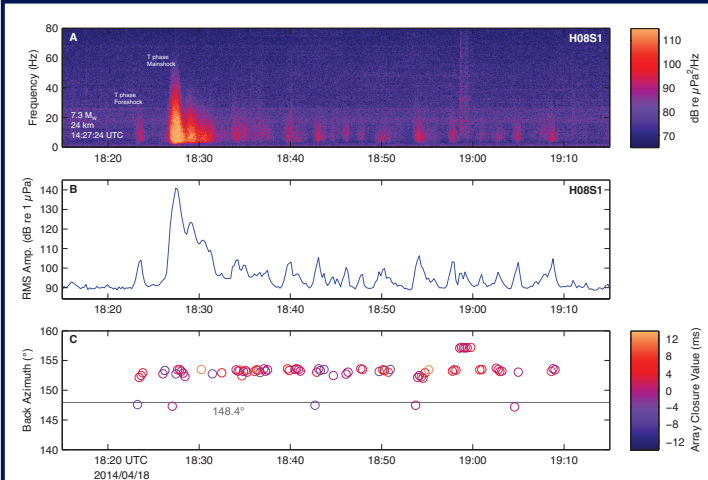
Introduction



(A-B) Location map and configuration of IMS hydrophone array H08S at Diego Garcia. The array (orange stars) is located 25 km south of the main island, with an equidistant inter-element spacing of 2 km. The mooring depth of ~1,400 m approximately corresponds to the axis of the SOFAR channel.

(C-D) Overview map of IMS station H08 (orange star), GEOSCOPE broadband seismometer TAOE at Marquesas Islands (red triangle), and the 2014 Guerrero earthquake epicenter (blue circle). The inset shows the location of the seismic mainshock along the Middle America Trench subduction zone (17.39°N, 100.97°W). Geodesic distances between the epicenter and the receiving stations are 21,354 km (H08S) and 5,195 km (TAOE). Bathymetry is taken from the GEBCO'08 grid.

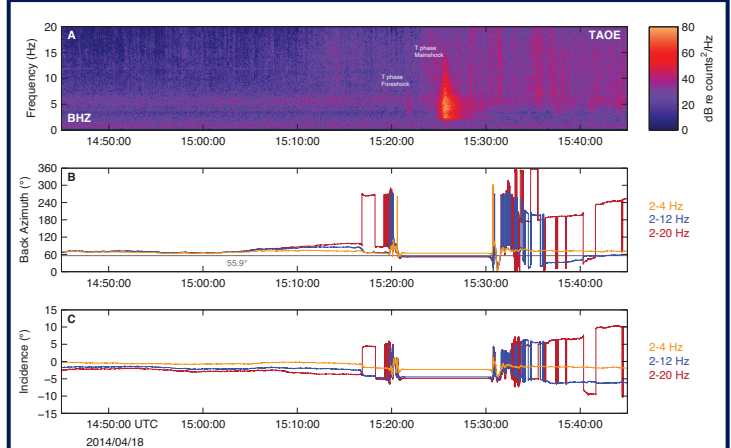
Hydroacoustic Observations



(A-B) 1-hour single-receiver spectrogram and 12-sec RMS amplitude of the H08S1 hydrophone data for T phase arrivals of the 2014 Guerrero earthquake. A 2 Hz high-pass filter is applied to eliminate low frequency noise. Wide-band contamination between 0 and 30 Hz is present due to air gun shooting and whale calls.

(C) Direction-of-arrival calculation for non-overlapping, 12-sec intervals [see Metz & Grevenmeyer 2018 for details]. The onset of the T phase corresponding to the mainshock is within ± 5 sec of the expected arrival time, assuming a celerity of 1480 m/s. Note that observed and geodesic (grey line) back azimuth differ by $\sim 4^\circ$. The signal may experience significant refraction due to horizontal temperature gradients at southern latitudes and near shallow bathymetric features, for instance in the vicinity of the Pitcairn Islands (see map above). Further uncertainty might be caused by the potential offset between epicenter location and seafloor-ocean coupling of seismic energy, an effect maximized at (near-)antipodal source-receiver ranges.

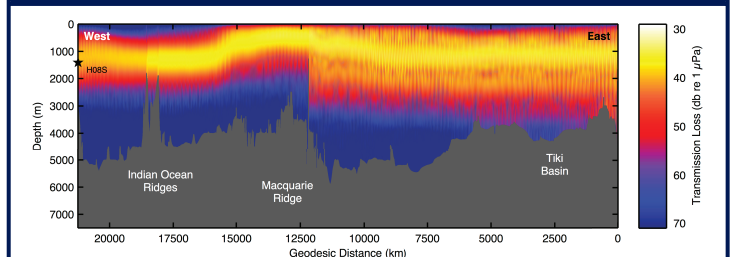
Seismic Data and Polarization Analysis



(A) 1-hour spectrogram of the vertical seismometer component at broadband station TAOE, Marquesas Islands. The data is recorded at 50 Hz sampling rate and high-pass filtered at 1 Hz. T phases associated with the 2014 Guerrero earthquake sequence are visible from approximately 15:23 UTC onwards, which is in agreement with the hydroacoustic observations at H08S. Note the identical offset between the fore and main shock arrival.

(B/C) Angle-of-arrival and vertical incidence for 300-sec windows (299.98-sec overlap) derived from polarization analysis [e.g. *Jurkevics, 1988*], implemented in the Polarizemic MATLAB Toolbox by *Haney & Mikesell* (<https://github.com/dylanmikesell/Polarizemic>). Three different band-pass filters are tested, with back azimuths distinctly stabilizing around the geodesic value (solid grey line). Signal incidence indicates a predominantly surface-type motion (horizontal measured from 0°). In both cases, waveform polarization appears to be surprisingly stable during the main arrival, but breaks down during the aftershock sequence, potentially due to the combined effect of reduced signal coherence and the relatively long analysis interval.

Transmission Loss Modelling



Range-dependent, 2D parabolic equation model (RAM, [Collins, 1993]) for a source-receiver path between the Middle America Trench and H08S (see solid line in top left figure). The model assumes an 8 Hz source at 50 m above the seafloor (1 km water depth) and does not account for the solid earth path before the coupling of acoustic energy at the seafloor-ocean interface. Transmission loss for a receiver (black star) at 1,400 m water depth is estimated to be ~ 42 dB re $1 \mu\text{Pa}$. Bottom properties are set to 1,700 m/s for sound speed, with attenuation parameters of 0.5 and 0.05 dB/m/kHz at 100 and 500 m below the seafloor, respectively.

Due to the temperature regime of the Antarctic Circumpolar Current (ACC), acoustic phases appear to propagate as surface reflected waves south of the 60°S parallel (approx. 10,000-15,000 km), thereby evading obstruction and reducing the effect of acoustic blockage near the Macquarie Ridge.

Summary

T phase arrivals at Diego Garcia (H08S) can be linked to earthquake activity along the Middle America Trench in the Pacific Ocean. These acoustic transmissions are the furthest to have ever been observed on Earth, exceeding 21,000 km in range.

Observations are confirmed by the analysis of broadband seismic data and transmission loss modelling.

Taking into account a larger dataset of suprapodal arrivals, future investigations may focus on the relationship between seismic and hydroacoustic magnitude, source depth, and seafloor-ocean coupling.

Key References

- Collins, M. D. (1993), A Split-Step Pade Solution for the Parabolic Equation Method, *J. Acoust. Soc. Am.*, 93(4), 1736-1742, doi:10.1121/1.406739.
- Jurkevics, A. (1988), Polarization analysis of three-component array data, *Bull. Soc. Am.*, 78 (5), 1725-1743
- Heaney, K. D., W. A. Kuperman, B. E. McDonald (1991), Perth-Bermuda sound propagation (1960): Adiabatic mode interpretation, *J. Acoust. Soc. Am.*, 90 (5), 2586-2594, doi: 10.1121/1.402062.
- Metz, D., A. B. Watts, I. Grevenmeyer, M. Rodgers, and M. Paulatto (2016), Ultra-long-range hydroacoustic observations of submarine volcanic activity at Monowai, Kermadec Arc, *Geophys. Res. Lett.*, 43, 1529-1536, doi:10.1002/2015GL067259.
- Metz, D., I. Grevenmeyer (2018), Hydroacoustic measurements of the 2014 eruption at Ahiy Volcano, 20.4°N Mariana Arc, *Geophys. Res. Lett.*, 45, 11,050-11,058, doi:10.1029/2018GL079983.